Non-metallic inclusions in aluminium killed steels

R. Dekkers, B. Blanpain, P. Wollants, F. Haers, C. Vercruyssen, and B. Gommers

Heats of medium carbon aluminium killed, low carbon silicon–aluminium killed, and low carbon aluminium killed steels were sampled with short time intervals during ladle metallurgy. Non-metallic inclusions were extracted from the steel matrix and investigated using scanning electron microscopy and energy dispersive spectrometry. Six inclusion morphologies were recognised, i.e. spherical, faceted, platelike, and dendritic shapes, as well as clusters and aggregates. For each sample also the total oxygen content was measured. Spherical inclusions were most abundant, but clusters, aggregates, and large faceted inclusions made up most of the oxide volume fraction. The present research shows that clusters, which are formed during the deoxidation operation, are removed within ~15 min after aluminium addition. Aggregates and large polyhedra appear after 5–10 min and their sizes increase with holding time. Small, mainly spherical and polyhedral, and to some extent also platelike, inclusions do not show evolution in size or in composition. I&S/1648

Dr Dekkers (rob.dekkers@mtm.kuleuven.ac.be), Professor Blanpain, and Professor Wollants are in the Department of Metallurgy and Materials Engineering, Katholieke Universiteit Leuven, Kasteelpark Arenberg 44, B–3001 Heverlee, Belgium and Dr Haers, Dr Vercruyssen, and Dr Gommers are with Sidmar N. V., John Kennedylaan 51, B–9042 Gent, Belgium. Manuscript received 11 September 2001; accepted 15 January 2002.

INTRODUCTION

Non-metallic inclusions in liquid aluminium killed steel consist mainly of aluminium oxides. If not captured by the slag, they can deteriorate the mechanical properties of the cast steel product. Moreover, they can disturb the continuous casting process.

Mainly two morphologies of non-metallic inclusions are observed in aluminium killed steels: aluminium oxide dendrites and clusters.[1–3] These have been observed both in laboratory experiments and in industrial practice. Faceted, platelike, and spherical inclusions have been reported as well. It has been found that the shapes of inclusions depend on the dissolved oxygen content, the concentration gradient of oxygen and aluminium in the liquid steel, the holding time, and the stirring method.[1–8]

The present work characterises inclusions from industrial heats of the Sidmar steelshop, documenting the types of inclusions present, and the evolution of inclusions during the ladle process. Heats of aluminium killed steels were sampled with short time intervals during ladle treatments. The non-metallic inclusions were extracted from the steel matrix and investigated in detail using scanning electron microscopy and energy dispersive spectrometry.

INDUSTRIAL PROCESS DESCRIPTION

After the converter process, steel contains 500–700 ppm of dissolved oxygen. It has to be deoxidised to prevent CO formation during casting. Deoxidation and adjustment of the final steel composition is carried out during ladle treatment. The ladle treatment at Sidmar starts with tapping of the converter, a basic oxygen furnace (BOF), holding 300 t of steel at ~1650°C. During tapping, alloying elements and deoxidation elements can be added, e.g. carbon, manganese, silicon, and aluminium. Next the slag, consisting of entrapped converter slag and deoxidation products, is skimmed and replaced by a synthetic slag that consists mainly of calcium oxide and, dependent on the steel composition, bauxite. The synthetic ladle slag has three functions, i.e. inclusion removal, thermal insulation, and prevention of atmospheric reoxidation. The final slag composition, after complete deoxidation of the steel, approximates to $12CaO.7Al_2O_3$, such that a low melting point liquid slag is obtained. Subsequently aluminium lumps are added, and the dissolved oxygen content of the steel is reduced to less than 5 ppm. The steel composition is finally adjusted by appropriate alloying. During deoxidation and alloying, the steel is stirred using argon or nitrogen. The secondary metallurgy treatment, from tapping until casting, takes ~95 min.

Standard steel sampling using dual samples (lollipops) to measure the chemical composition is carried out after tapping, after killing, and at the end of the secondary metallurgy treatment.

STEEL SAMPLING

Samples of the liquid steel were taken by using a total oxygen sampling (TOS) device.[9] The small diameter of such a sample (4 mm) ensures fast cooling, and therefore the inclusions in the sample are representative of the melt at the moment of sampling. Automatic sampling was carried out such that the location of sampling, 20 cm below the slag surface and very close to the centre of the ladle, was constant.

Heats of medium carbon aluminium killed (MCAK), low carbon silicon–aluminium killed (LCSAK), and low carbon aluminium killed (LCAK) steels were sampled with short time intervals. The compositional ranges of the steel grades are listed in Table 1. For every steel grade two heats were sampled.

Table 1 Compositional ranges of investigated steel grades,* ppm

	C	Si	Mn	P	Al	Fe
MCAK	1100–1400	0–200	5500–6000	0–180	150–550	Bal.
LCSAK	0–450	2000–2600	6200–7700	0–200	150–300	Bal.
LCAK	250–450	0–200	1500–2300	0–120	300–650	Bal.

*MCAK is medium carbon aluminium killed, LCSAK is low carbon silicon–aluminium killed, LCAK is low carbon aluminium killed.

EXTRACTION OF INCLUSIONS

Extraction of inclusions from a steel allows the morphology of the inclusions to be described in detail. In the present work, the extraction procedure was based on a standard test method to determine the acid insoluble content of copper and iron powders (ASTM standard E194–90).[10] The method is inappropriate in the case of sulphides, silicates, and calcium aluminates. A steel sample of ~3 g were ground with silicon carbide paper to remove surface oxides, and dissolved into a 100 mL aqueous solution of hydrochloric acid (1:1) under heating (80–100°C). After ~3 h all iron had dissolved and 150 mL of hot deionised water was added. The hot iron solution was filtered over a Nuclepore membrane with pores of 0·2 μm. The residue was washed alternately with a hot (close to boiling) aqueous solution of hydrochloric acid (1:25) and hot deionised water, five times each. The washing should ensure the removal of all iron salts. The Nuclepore membrane was used because of its resistance to acid and its flat surface that facilitates investigation by scanning electron microscopy (SEM).

SPECIMEN PREPARATION AND ANALYTICAL TECHNIQUES

The extracted non-metallic inclusions were coated with carbon, because the inclusions and the membrane were non-conductive. Carbon instead of gold or silver was chosen to enhance the detection of light elements, e.g. oxygen and magnesium, by energy dispersive spectrometry (EDS).

High resolution SEM was carried out using Philips XL30 field emission gun (FEG) apparatus, equipped with an EDS detector (EDAX) with an ultrathin window, which enables detection of elements starting from boron. For calculation of elemental composition, EDAX software was used applying a phi–rho–Z correction.

CLASSIFICATION OF INCLUSIONS

Inclusions present after aluminium addition consisted of pure aluminium oxide or aluminium oxide with small amounts of magnesium (commonly less than 4 at.-%). Occasionally traces of manganese, silicon, and/or calcium were also detected. In LCSAK steel, manganese silicates were observed before the addition of aluminium. Non-metallic inclusions can be classified by shape, chemical composition, or size. In the present study, classification was based on shape. Six inclusion types were recognised.

1. Spherical inclusions:
   (i) small, nearly perfect spherical aluminium oxides with an average diameter of 0·5 μm (Fig. 1*A*)
   (ii) large spherical inclusions with an average diameter of 2·6 μm. Frequently small amounts of manganese or silicon were detected. These inclusions were observed only in LCSAK steel.
2. Faceted inclusions:
   (i) octahedral inclusions with an average size of 2·4 μm, almost always containing magnesium, at an average level of 2·1 at.-% (Fig. 1*B*)
   (ii) small polyhedral (non-octahedral) inclusions, i.e. faceted particles not showing an octahedral tendency. They were defined as being smaller than 5 μm (2·7 μm on average), and usually contained magnesium (2·1 at.-% on average) (Fig. 1*C*)
   (iii) large polyhedral inclusions, defined as being larger than 5 μm, consisting of pure aluminium oxide (Fig. 1*D*).
3. Platelike inclusions, mainly hexagonal or trigonal. Occasionally rectangular plates were observed. Their average length was 2·9 μm, and sometimes magnesium (1·7 at.-% on average) was detected (Fig. 1*E*). Their thickness was estimated to be less than 0·1 μm.
4. Dendrites consisting of pure aluminium oxide. The primary branches were commonly oriented in a trigonal manner. Their sizes ranged from 5 to 20 μm (Fig. 1*F*).
5. Clusters form an open network of aluminium oxides. Individual particles were often unrecognisable, and facets were absent or only weakly developed (Fig. 1*G*). Their longest diameter could be over 100 μm.
6. Aggregates consisting of an accretion of faceted particles (Fig. 1*H*). Commonly magnesium was not detected in aggregates, but occasionally particles in aggregates contained magnesium. The longest diameter of aggregates could be up to a few tens of micrometres.

Table 2 lists average size measurements and magnesium contents, as well as standard deviations of the sample averages. Inclusions varied in magnesium content and in size. Magnesium bearing inclusions were octahedral, small polyhedral, and platelike inclusions. With respect to size three groups were recognised, i.e. (a) large polyhedra, aggregates, and clusters, (b) large spheres, octahedra, small polyhedra, and platelike inclusions, and (c) small spheres. Dendrites are not considered further, because they were observed only rarely.

EVOLUTION OF INCLUSIONS

Large inclusions are considered to be most detrimental. In the present work they occurred as clusters, aggregates, and large polyhedra (> 5 μm), and sometimes as dendrites. Figure 2 shows the average sizes of clusters, agglomerates, and large polyhedra versus time after aluminium addition. In every sample the average sizes were determined from at least 15 measurements in the case of clusters, and at least five measurements in the cases of aggregates and large polyhedra, which were often scarce and therefore difficult to detect. It can be seen that after ~10 min clusters had disappeared; only small aggregates and large polyhedra remained, independent of the heat. The largest clusters were observed a few minutes after aluminium addition, with large variations in size of the clusters. Clusters in LCAK and MCAK steels seemed to be slightly larger than clusters in LCSAK steels. The size (longest diameter) of the aggregates and polyhedra slowly increased during ladle treatment.

Small polyhedra were smaller than 5 μm. They usually contained small amounts of magnesium. A special type of

Table 2 Average magnesium contents and sizes of given inclusion shapes: number of analyses/measurements and standard deviations τ are also listed

	Mg content			Size		
	Number	Average, at.-%	σ, at.-%	Number	Average, μm	σ, μm
Small spherical	889	0·85	0·25	8980	0·53	0·26
Large spherical	93	0·70	0·17	102	2·58	0·92
Octahedral	611	2·14	0·87	613	2·41	0·73
Non-octahedral	736	2·06	1·06	696	2·70	0·79
Platelike	602	1·68	0·84	572	2·85	1·55
Cluster	225	1·18	1·38	427	59·6	44·5
Aggregate	300	1·29	1·08	557	13·4	15·1
Large polyhedral	93	0·79	0·31	106	7·87	7·43

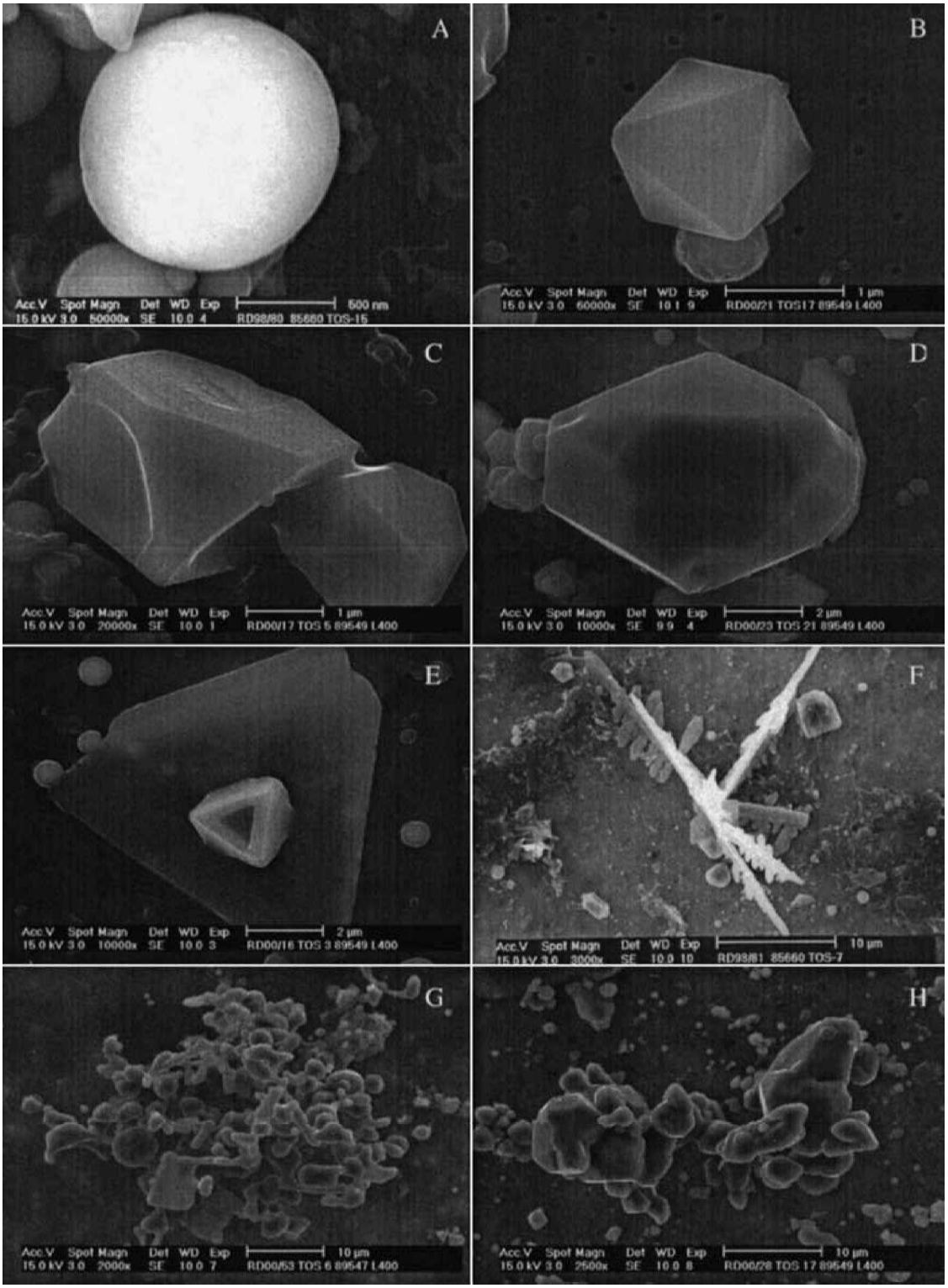

A small spherical inclusion; *B* octahedral inclusion; *C* small polyhedral inclusion; *D* large polyhedral inclusion; *E* platelike inclusion; *F* dendrite; *G* cluster; *H* aggregate

1 Typical inclusion shapes: inclusions have been extracted from steel matrix

polyhedron is the octahedron. Since corundum, the most stable aluminium oxide, has a hexagonal symmetry, the octahedra in the present work were clearly not corundum. Therefore they were analysed separately. In every sample at least five inclusions were measured to determine the average size. Figure 3 shows the average sizes and magnesium contents in both octahedral and non-octahedral inclusions. Obviously no significant change in size or magnesium content of small polyhedra occurred with time after aluminium addition. Discrimination between small polyhedra (non-octahedra) and octahedra was not always easy.

Platelike inclusions varied a lot in size and in magnesium content. Most were hexagonal, but trigonal and sometimes rectangular shapes were observed as well. Their thickness varied from very thin films to thicker plates.

Two types of spherical inclusions were observed. Most were rather small, $\sim 0{\cdot}5$ μm, and consisted of almost pure

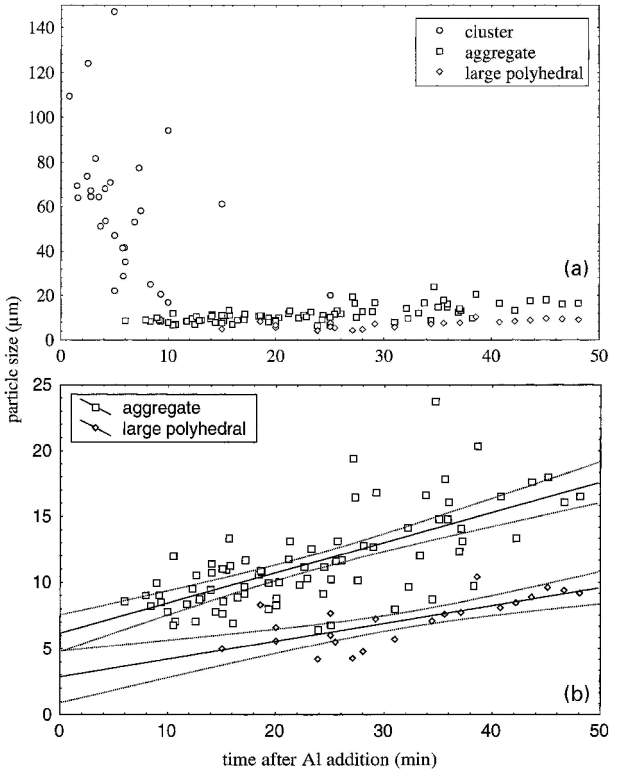

2 *a* Average sizes of clusters, aggregates, and large polyhedra versus time after aluminium addition in all three steel grades, and *b* increase in size of aggregates and large polyhedra in all heats: linear fits and 95% confidence bands are indicated

aluminium oxide. In samples taken from LCSAK steels before killing, spherical SiO_2 inclusions were indentified after extraction. Investigation of polished steel surfaces of these samples revealed the presence of spherical $MnSiO_3$ inclusions. Therefore it was concluded that $MnSiO_3$ transformed to SiO_2 during the hydrochloric acid dissolution. Larger, 2–5 μm, spherical aluminium oxide inclusions with small amounts of manganese and silicon were also observed. Figure 4 shows the average size (50 measurements) of the abundant pure aluminium oxide inclusions measured in every sample taken during ladle treatments of the six heats. No significant effect of ladle treatment time on size was observed. Although the number of inclusions was not counted systematically, SEM observations suggested that it decreased with time.

RELATIVE PRESENCE OF INCLUSION SHAPES

The relative presence (%) of inclusion shapes was derived by classification of 500 randomly selected inclusions per sample (Table 3). Results from two heats for every steel grade were averaged. Samples taken immediately after aluminium addition were not included because they contained mainly very large clusters (up to hundreds of micrometres), making discrimination between clusters and isolated inclusions very tedious. Small spherical inclusions were by far the most abundant, representing 87–98% of the total number of inclusions.

To compare the relative presence of the various inclusion types, the volume of inclusions must be considered. For instance, 1 ppm oxygen in a 1 g steel sample can be caused by one aluminium oxide particle of ~100 μm or by 10^9 particles of 0·1 μm in diameter. The relative importance of the different types of inclusions with respect to oxidic oxygen was derived from the results given in Table 3, assuming average volumes for all inclusion types. The average sizes of the various types of inclusions are listed in Table 2. Volumes for the octahedral and non-octahedral shapes was derived by assuming octahedrons with body diagonals equal to the average maximum lengths. Platelets were considered as trigonal plates with a thickness of 0·1 μm. The volume related to a cluster was estimated to be 3% of the volume of a sphere enveloping the cluster.[11] Volumes of aggregates and large polyhedra were associated with tetragonal prisms with bases 5 μm × 5 μm × average lengths. Dendrites were considered as tubes with radius 0·5 μm and length 10 μm. With the aforementioned assumptions, the average volumes of inclusions were calculated. The results listed in Table 4 reveal that the average volumes of the various inclusion types may differ by a factor of 10^5.

With respect to the evolution of non-metallic inclusions with holding time, the sizes of clusters, aggregates, and large polyhedra were made time dependent (Table 5), the expression for time dependence derived from Fig. 2*a*. Although derivation of volume per inclusion type was indirect, Table 5 clearly indicates that the large inclusions, i.e. clusters, aggregates, and large polyhedra, if present, contained the majority of oxidic oxygen in the liquid steel, i.e. 59–100%. Furthermore, non-octahedral and small spherical inclusions represented a significant degree of oxidic oxygen in some cases.

TOTAL OXYGEN CONTENT

A part of every TOS sample was used for two total oxygen (O_{tot}) measurements in the cases of MCAK and LCAK steels, and for one in the case of LCSAK steel. The O_{tot} values versus time after aluminium addition are plotted in Fig. 5. The scatter of results was large up to 15 min after

Table 3 Relative presence of given inclusion shapes observed during ladle metallurgy, %

	Small spherical	Large spherical	Octahedral	Non-octahedral	Platelike	Cluster	Aggregate	Large polyhedral	Dendritic
MCAK									
10 min	93	...	0·3	3·0	3·0	0·3	...	...	0·2
20 min	97	...	0·1	1·3	1·3	...	0·1	...	0·1
30 min	90	...	0·4	6·5	0·8	...	1·6	...	0·2
40 min	92	...	0·2	5·4	1·8	...	0·2	...	0·4
LCSAK									
10 min	89	1·8	1·6	5·3	1·3	...	0·6	...	...
20 min	96	0·2	0·5	2·6	0·6	...	0·1	...	...
30 min	92	0·5	0·3	3·6	2·5	...	0·7	...	0·1
40 min	87	...	0·3	6·6	5·2	0·1	0·4	0·1	0·1
50 min	90	0·2	...	2·2	6·6	...	1·2	...	...
LCAK									
5 min	93	...	1·4	1·0	1·3	3·7	...	...	0·1
10 min	95	...	0·5	0·5	1·2	2·5	...	...	0·2
15 min	96	...	0·3	2·1	1·3	...	0·4	...	...
20 min	98	...	0·5	1·1	0·3	...	...	...	...
25 min	97	...	0·3	1·3	0·5	0·1	0·1	0·1	0·2

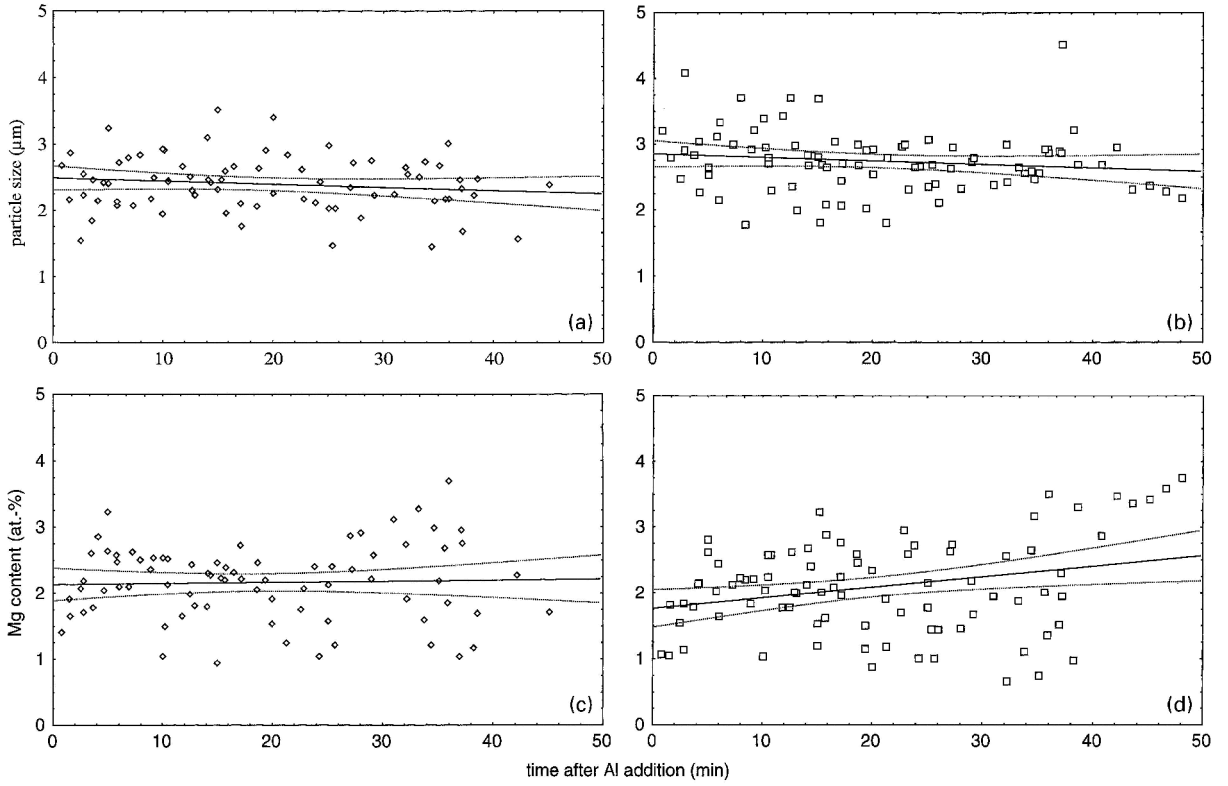

a size, octahedra; *b* size, non-octahedra; *c* Mg content, octahedra; *d* Mg content, non-octahedra

3 Average sizes and magnesium contents in small polyhedra versus time after aluminium addition: linear fits and 95% confidence bands do not indicate significant changes

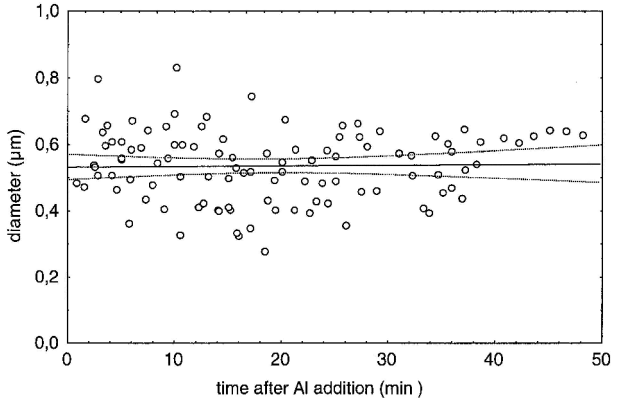

4 Average size of small spherical inclusions: linear fit and 95% confidence bands indicate no evolution

aluminium addition. This is explained by the statistical presence of clusters in the samples. Clusters contained most of the bonded oxygen, and were removed from the steel within ~15 min after aluminium addition. The O_{tot} of any heat remained approximately constant after 15 min.

Table 4 Average volumes of inclusions

Type	Volume, m^3
Small spherical	$7{\cdot}71 \times 10^{-20}$
Large spherical	$8{\cdot}99 \times 10^{-18}$
Octahedral	$2{\cdot}33 \times 10^{-18}$
Non-octahedral	$3{\cdot}28 \times 10^{-18}$
Platelike	$3{\cdot}50 \times 10^{-19}$
Cluster	$3{\cdot}33 \times 10^{-15}$
Aggregate	$3{\cdot}35 \times 10^{-16}$
Large polyhedral	$1{\cdot}97 \times 10^{-16}$
Dendritic	$7{\cdot}85 \times 10^{-18}$

DISCUSSION

Detailed investigation of non-metallic inclusions extracted from industrial steel samples indicates that, for all steel grades, six main morphology types of inclusions occur: spherical, polyhedral, and platelike, and dendrites, clusters, and aggregates. The spherical inclusions are subdivided into two subtypes, which differ in size and in composition. Polyhedral inclusions are subdivided into octahedral, non-octahedral, and large polyhedral particles. Spherical inclusions are most abundant throughout the secondary metallurgy process, but clusters, aggregates, and large polyhedra (>5 μm) contain most of the oxidic oxygen owing to their large sizes. Non-octahedral and spherical inclusions may account for significant oxygen as well. Since large inclusions are considered as being most harmful, the O_{tot} measurements indicate indeed the presence of potentially detrimental inclusions. It must be noted here that if

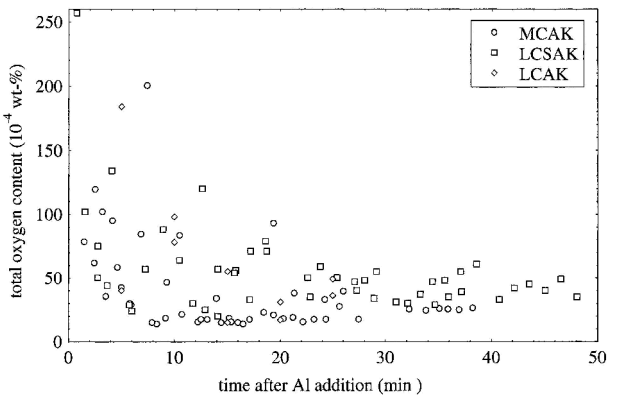

5 Total oxygen contents in low carbon silicon–aluminium killed (LCSAK), medium carbon aluminium killed (MCAK), and low carbon aluminium killed (LCAK) steels: two heats each

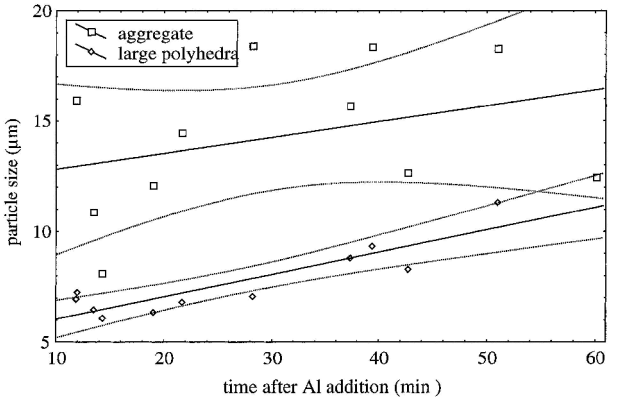

6 Evolution of sizes of aggregates and large polyhedra from a number of LCAK heats versus time after aluminium addition

only a few large clusters are present in the ladle, they may not be sampled by the TOS process. Steels with extremely low oxygen contents can be produced only if clusters, aggregates, and large polyhedra are removed efficiently.

Long holding times of ladles are usually considered to be favourable, because inclusions are allowed to float into the slag. The present study shows that clusters formed during deoxidation disappear within ~15 min after aluminium addition. Other researchers[2,3,12] have also observed the fast removal of large inclusions. However, aggregates and large polyhedra, which were not observed in samples taken within the first minutes after aluminium addition, increase in size from ~5 to 20 μm at the end of the secondary metallurgy treatment (Fig. 2). A similar evolution of large inclusions was observed in LCAK steels (Fig. 6). The presence of particles similar to small faceted inclusions suggests that the growth of agglomerates occurs mainly by attachments of single inclusion particles. The increase of size of aggregates and large polyhedra indicates that coalescence of non-metallic inclusions may play an important role in the formation of large detrimental particles. Small inclusions, mainly spherical and polyhedral particles and to a lesser extent platelets, do not show evolution either in size or in composition.

Since O_{tot} during ladle treatment remains about constant after the removal of the largest inclusions, it is supposed that a dynamic equilibrium is established. The equilibrium implies a balance between inclusion removal and reoxidation. The driving force for the formation of new particles is considered to be too low, because of the high number of inclusions present in the steel bath, which will act as growth sites. Indications of inclusion growth were the formation of dendrite tips on existing particles and overgrowth (Fig. 7). However, the change in size was too small to be measured. Growth of aggregates is mainly by attachment of particles, and is therefore different in nature.

During secondary metallurgy treatment, a significant loss of dissolved aluminium content may take place, attributed to oxidation of the dissolved aluminium. Since this oxidation is related to interfacial reactions, e.g. steel–slag, the aluminium loss is not necessarily related to the growth of oxide inclusions only.

From the start of secondary metallurgy treatment up to casting, the liquid steel temperature drops by ~50 K. Decreased oxygen solubility of the steel causes precipitation

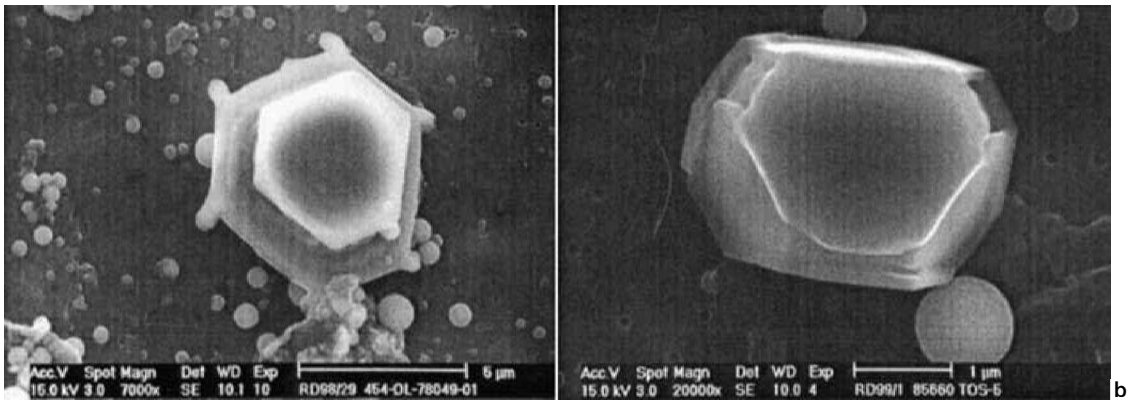

a b

a formation of dendrite tips; *b* overgrowth

7 Growth of inclusions during secondary metallurgy treatment

Table 5 Volume fraction of bonded oxygen per inclusion type based on data in Table 3: estimated volume of single particle is given in Table 4, sizes of clusters, aggregates, and large polyhedra are time dependent, i.e. $74{\cdot}975\exp(-0{\cdot}059t)$, $6{\cdot}158+0{\cdot}229t$, and $2{\cdot}862+0{\cdot}134t$, respectively (t in min)

	Small spherical	Large spherical	Octahedral	Non-octahedral	Platelike	Cluster	Aggregate	Large polyhedral	Dendritic
MCAK									
10 min	0·3	...	0·0	0·4	0·0	99	0·0	...	0·1
20 min	19	...	0·6	11	1·1	...	67	...	2·0
30 min	1·3	...	0·2	3·9	0·1	...	94	...	0·3
40 min	6·7	...	0·4	17	0·6	...	73	...	3·0
LCSAK									
10 min	4·0	10	1·8	10	0·2	...	74	...	...
20 min	16	3·9	2·5	19	0·3	...	59	...	...
30 min	2·8	1·8	0·3	4·7	0·2	...	90	...	0·3
40 min	3·2	...	0·3	10	0·5	21	73	10	0·4
50 min	1·3	0·3	...	1·3	0·3	...	97	...	...
LCAK									
5 min	0·0	...	0·0	0·0	0·0	100	...	...	0·0
10 min	0·0	...	0·0	0·0	0·0	100	...	...	0·0
15 min	6·7	...	0·6	6·2	0·2	...	86	...	...
20 min	61	...	9·4	29	0·5	...	...	...	...
25 min	6·1	...	0·6	3·5	0·1	52	24	13	1·3

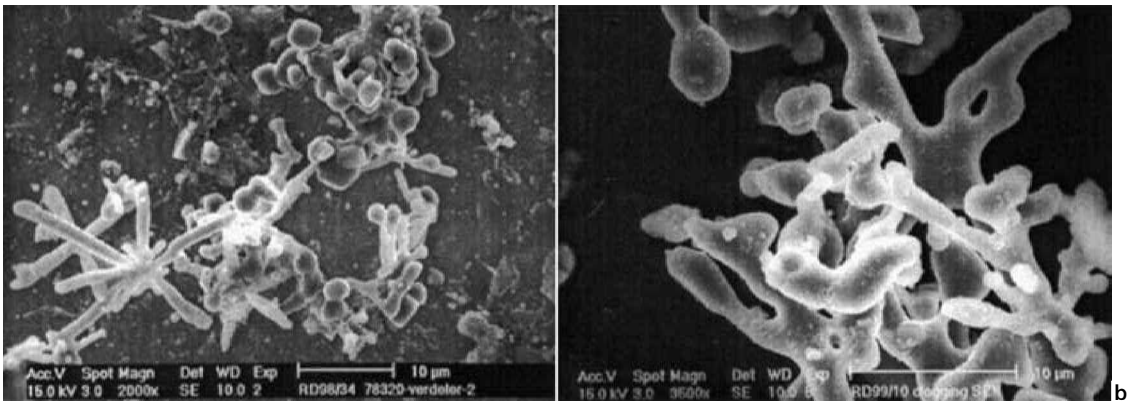

a cluster partially built up by dendrites in tundish; *b* clusters from clogging material

8 Different types of clusters

of aluminium oxide. Considering a slow temperature decrease, precipitation will occur on existing inclusions. To estimate the influence of cooling of the steel on inclusion growth, the effect of precipitation of aluminium oxide from the steel has been calculated. For simplicity, only spherical inclusions have been considered with initial diameters of 0·5 and 10 μm. The liquid steel contains 30 ppm oxygen in total, of which 25 ppm oxygen is bonded in aluminium oxide inclusions and 5 ppm oxygen is dissolved in the melt. Decreasing the dissolved oxygen to 2 ppm results in growths (in diameter) of 0·02 and 0·38 μm in the cases of 0·5 and 10 μm sized inclusions, respectively. This simple calculation shows that growth owing to cooling is hardly detectable from size measurements.

Despite the removal of clusters at the end of the ladle treatment, some aluminium oxides in the tundish and in the nozzle clogging material will be present as clusters. Collisions and subsequent attachments of inclusions will produce aggregates, but the rounded surfaces of clusters are more probably a result of severe cooling or reoxidation, which implies larger growth rates (Fig. 8). Therefore, the problem is not only how to obtain clean steel by secondary metallurgy treatment, but also how to keep the steel clean thereafter. The effects of tundish and mould slag, and oxygen leaks along the nozzles, should be considered, but are outside the scope of the present research.

Interactions between liquid steel and slag and/or refractory materials may result in the formation of new inclusions, or in the presence of typical slag or refractory components in inclusions. Particles originating from the refractory material differ much from normal inclusions (Fig. 9). They are large, and show typically shell fracture shaped surfaces (Fig. 9*a*). They were observed on only a few occasions during the present research. Therefore, their presence is considered to be negligible in the overall picture. No slag particles were observed.

Low levels of magnesium (1–4 at.-%) were detected in small faceted and in platelike inclusions. This suggests that these inclusions form differently, compared with spherical particles and clusters. Refractory and slag can be sources of magnesium. Magnesia refractory is present only in the slag zone of the ladle lining. Another potential source of magnesium is the aluminium added for deoxidising the steel, which contains ~0·5 wt-% magnesium. Supposing that all aluminium reacts to form aluminium oxide, and that magnesium is dissolved in the newly formed aluminium oxide, then ~7·5 wt-% of the inclusions can contain 3 at.-% magnesium. Since the volume fraction of faceted and platelike inclusions is negligible compared with the volume of clusters, the magnesium content of the aluminium lumps used for deoxidation of the steel can indeed account for the magnesium detected in small polyhedral and platelike aluminium oxide inclusions. The presence of small amounts of magnesium in certain inclusion types may be related to their kinetics of formation or to their ability to incorporate magnesium.

Octahedral inclusions and small amounts of magnesium in some inclusion types indicate that aluminium oxides other than corundum may be present in the liquid steel. Indeed, such phases have been found.[13–15] It is supposed that overgrowth of octahedra occurs, which gives rise to non-octahedral inclusions (small polyhedra). The hypothesis of overgrowth is supported by the observation that the frequency of non-octahedral inclusions increases with time, while that of octahedral inclusions decreases. Moreover, small polyhedra are generally larger than octahedra.

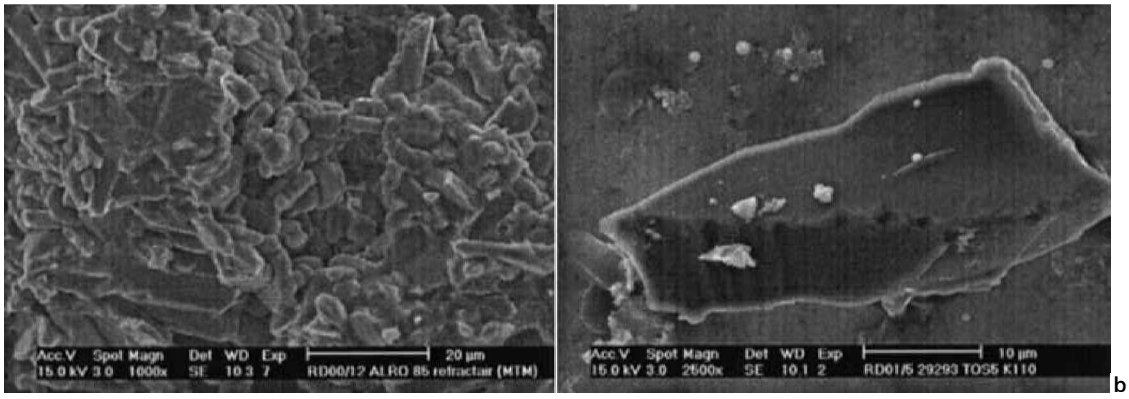

a surface of fresh fault in unused aluminium oxide refractory; *b* aluminium oxide particle found in steel sample

9 Different types of particles

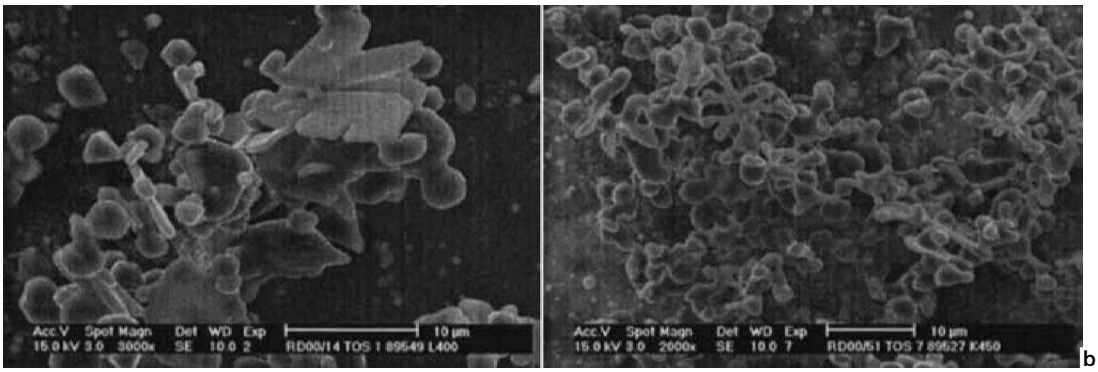

10 In LCSAK steel clusters consist more of faceted and platelike inclusions, *b* those in LCAK and MCAK steels have more dendrite–aggregate character with almost no facets

Calcium was less frequently measured than was magnesium in inclusions. In MCAK and LCSAK steels inclusions containing calcium were exceptionally rare, but in LCAK steels they were detected more commonly. Just as for magnesium, the calcium concentration reached approximately 1–3 at.-%. Calcium was detected in all types of inclusions. Calcium is a typical slag component. So far, it is unclear why calcium was detected more frequently in the LCAK grade than in the MCAK and LCSAK grades.

Before deoxidation, manganese silicate inclusions were observed in LCSAK steels. These inclusions are liquid at steelmaking temperatures. They are reduced by aluminium resulting in large, generally 2–5 μm, spherical aluminium oxide particles, which frequently contain small amounts of silicon and/or manganese as well. Since a part of the oxygen present in the liquid steel is bonded in manganese silicates before the addition of aluminium, less dissolved oxygen may be available to react with aluminium at the moment of aluminium addition than in the case of LCAK steels. Therefore the kinetics of inclusion growth may be slower, which can result in more faceted particles. This may explain why the clusters consist more of faceted and platelike inclusions in LCSAK steels, in contrast with clusters in LCAK and MCAK steels that have a more dendrite–aggregate character with almost no facets (Fig. 10). Braun *et al.*[6] found a very similar effect for clusters formed in iron melts with different oxygen contents.

CONCLUSIONS

Total oxygen samples of medium carbon aluminium killed, low carbon silicon–aluminium killed, and low carbon aluminium killed steels were taken to characterise the type of inclusions and their evolution during secondary metallurgy treatment. With respect to size and composition, spherical, platelike, and small polyhedral inclusions were approximately constant in the six heats investigated. Evolution in size of large inclusions was observed. Clusters were present within the first 10 min after aluminium addition. After 15 min aggregates and large polyhedra arose and increased continuously in size. The formation of aggregates and their subsequent growth are attributed to the attachment of single particles whenever inclusions met.

Small spherical inclusions could account for 90% or more of the number of inclusions throughout the secondary metallurgy treatment. However, large inclusions represented from 59 to almost 100% of the oxide volume. The oxygen content related to the abundant but small spherical inclusions was almost negligible. Since most oxygen was present in the large inclusions, generally considered to be most detrimental for global steel quality, the oxygen content was a measure of the steel quality in the heats investigated (provided that the steel samples were representative of the steel bath).

If only the flotation of inclusions is considered, increasing the holding time of the ladle should improve steel cleanliness. However, since aggregates and large polyhedra increase in size during the secondary metallurgy treatment, it is suggested that the cleanest steel, with respect to inclusion size, is obtained at ~15 min after deoxidation.

ACKNOWLEDGEMENT

This research has been funded by the IWT project 99–0251.

REFERENCES

1. E. STEINMETZ, H.-U. LINDENBERG, W. MÖRSDORF, and P. HAMMERSCHMID: *Arch. Eissenhüttenwes.*, 1977, **48**, 569–574.
2. W. TIEKINK, J. BROCKHOFF, and J. VAN DER STEL: Proc. 4th Int. Conf. on 'Clean steel', Balatonszéplak, Hungary, 1992, Hungarian Mining and Metallurgical Society, 704–717.
3. W. TIEKINK, A. PIETERS, and J. HEKKEMA: *Iron Steelmaker*, 1994, **21**, (7), 39–41.
4. E. STEINMETZ and H.-U. LINDENBERG: *Arch. Eissenhüttenwes.*, 1976, **47**, 199–204.
5. E. STEINMETZ, H.-U. LINDENBERG, W. MÖRSDORF, and P. HAMMERSCHMID: *Stahl Eisen*, 1977, **97**, 1154–1159.
6. T. B. BRAUN, J. F. ELLIOTT, and M. C. FLEMINGS: *Metal. Trans. B*, 1979, **10B**, 171–184.
7. E. STEINMETZ, H.-U. LINDENBERG, P. HAMMERSCHMID, and W. GLITSCHER: *Stahl Eisen*, 1983, **103**, 539–545.
8. E. STEINMETZ and C. ANDREAE: *Steel Res.*, 1991, **62**, (2), 54–59.
9. A. JUNGREITHMEIER, A. VIERTAUER, H. PRESSLINGER, and K. ANTLINGER: *Radex Rundsch.*, 1993, **3/4**, 369–387.
10. Standard E194–90, 'Annual book of ASTM standards', Vol. 03.05, 428; 1992, Philadelphia, PA, ASTM.
11. Y. MIKI, Y. SCHIMADA, B. G. THOMAS, and A. DENISSOV: *Iron Steelmaker*, 1997, **24**, (8), 31–38.
12. M. JEFFORD, G. BETKA, S. MCINTOSH, AND L. D. WAY: Proc. 3rd Int. Cong. on 'Oxygen steelmaking', Oct.–Nov. 2000, Birmingham, UK, Iron and Steel Division, The Institute of Materials, 307–317.
13. A. ADACHI, N. IWAMOTO, and M. UEDA: *Trans. Iron Steel Inst. Jpn*, 1966, **6**, 24–30.
14. R. G. SMERKO and D. A. FLINCHBAUGH: *J. Met.*, 1968, **20**, (7), 43–51.
15. R. DEKKERS, P. WOLLANTS, B. BLANPAIN, F. HAERS, C. VERCRUYSSEN, and B. GOMMERS: Proc. 2nd Int. Cong. on 'The science and technology of steelmaking', Swansea, UK, April 2001. The Institute of Materials, 655–665.